A Simulation Study of Sensor Behavior for Non-Invasive Electrical Resistance Tomography

Yasmin Abdul Wahab*[1], Nur Faten Faseha Hisham[1], Maziyah Mat Noh[1], Zainah Md. Zain[1], Normaniha Abd Ghani[1], Mohd Anwar Zawawi[1]. Muhammad Sharfi Najib[1], and Ruzairi Abdul Rahim[2]

[1]*Faculty of Electrical and Electronics Engineering Technology, Universiti Malaysia Pahang, 26600 Pekan, Pahang, Malaysia,*
[2]*School of Electrical Engineering, Faculty of Engineering, Universiti Teknologi Malaysia, 81310 Skudai, Johor Bharu, Malaysia*

Corresponding author email: yasmin@ump.edu.my

Abstract

The non-invasive method is one of the common methods applied in process plants, compared to other sensing methods. The paper aims to investigate the feasibility study of sensor behaviour implemented in non-invasive Electrical Resistance Tomography (ERT) by applying various materials and shapes for electrodes. Based on a quasi-static electric field, a 3D simulation using finite element model software (COMSOL Multiphysics) was applied to investigate and analyse the sensor behaviour. A 100 mm outer diameter and 2 mm thick acrylic pipe was used for the non-invasive ERT system. A studying of a fringe effect also was the focus in this project. Thus, it is believed that the implementation material such as copper and steel, circle shape and the fringe effect of the electrode could allow the electricity to be emitted and detect significantly. The non-invasive of ERT system would also gave an alternative way for industry to monitor the performance of the process plants.

Keywords: ERT, sensor behaviour

1. Introduction

Tomography systems are suitable for applications requiring non-invasive and non-intrusive monitoring systems, especially in industries that deal with the multiphase flow. Originally, the term 'tomography' comes from the Greek language, 'Tomos' which means cutting section and 'graph' which means image or picture [1]. Otherwise, tomography can be defined as a method to reconstruct the image of the object's interest within the sensing zone [2]. Besides electrical resistance tomography (ERT) imaging method; there are also apply electrical capacitance

tomography (ECT), electrical impedance tomography (EIT), x-ray tomography, ultrasonic tomography and optical tomography. Moreover, tomographic techniques are concern with abstracting information to form a cross sectional image and the derivation of an information relating to two or three dimensions.

Process tomography uses several sensing methods approaches to reveal complexities of internal structure of an object without the need to occupy it. There are four types of sensing methods for tomography; intrusive, non-intrusive, invasive and non-invasive. Thus, based on the principles of process tomography chosen, the researchers should know which method is suitable or fit for the process tomography system.

In the past decades, non-invasive method proved it is bring benefits and more advantages for the industry compared to other sensing methods [3]. The advantages of the non-invasive method are it gains limiting the safety and accountancy troubles with important process materials, assisting installation (and even retrofitting) and caring for the instruments even when the plant is on-stream, keeping away from contamination of pure or sterile materials, and finally, decreasing the hazards of working with poisonous, radioactive, explosive, flammable or corrosive materials [4].

Electrical resistance tomography (ERT) is a large-scale procedure of process tomography that being applied and has many applications such as it is applied for geological surface [5], agriculture processes [6] and industrial processes [7]. The effects of using the ERT is safe and provide fast response for an online and real-time monitoring. Moreover, the examples of ERT in identifying a medium of interest are liquid-liquid, liquid-gas, or liquid-gas mixtures. Therefore, a non-invasive of electrical resistance tomography (ERT) for studying its sensor behaviour using simulation approach is a focus in this paper.

2. Problem Background

Electrical Resistance Tomography (ERT) is applied non-intrusive to the system. The suitableness of ERT to dense particulate systems was already determined in a very range of works [6], moving from preliminary qualitative investigations based on the visual observation of the measured conductivity to, the quantitative analysis of different variables. Here, the concentration distribution of the dispersed phase is the most generally explored. In other works,

electrical resistance tomography investigated the experiment liquid mixing in a solid-liquid baffled stirred tank [8].

The following are the problems that need to be considered in the studying of sensor behavioural in a non-invasive electrical resistance tomography:

i.   The implementation of an non-invasive ERT system in industrial is less [9]. This is because the effect of electrodes on the nature of the process flow.

ii. Usually, the researchers used copper material for electrodes, and the shape of electrodes is rectangular [10], [11]. To study the feasibility behaviour of the sensor because the contact between metal electrode and conductive liquid can produce a chemical reaction.

3. Basic Principles of ERT

Electromagnetic field theory mainly the Maxwell's equations were enforced as a basis principle within the electrical tomography system. The field and therefore the medium of interest can influence the field of the electrical tomography system to be an associate electrostatic field, electromagnetic field, or electro quasi-static (EQS) field. Hence, the Maxwell equations [12] are represented as follows:

$$\nabla . \boldsymbol{D} = \rho \text{ (Gauss Law)} \tag{1}$$

$$\nabla . \boldsymbol{B} = 0 \text{ (Gauss Law)} \tag{2}$$

$$\nabla x \boldsymbol{H} = \boldsymbol{J} + j\omega \boldsymbol{D} \text{ (Ampere's Law)} \tag{3}$$

$$\nabla x \boldsymbol{E} = 0 \tag{4}$$

Where

$\boldsymbol{D}$ = the electric flux density,

$\boldsymbol{E}$ = the electric field intensity,

$\boldsymbol{J}$ = the current density,

ρ = the free charge density,

$\boldsymbol{B}$ = the magnetic flux density,

$\boldsymbol{H}$ = the magnetic field intensity and ω is the angular frequency.

Moreover, the relationship between $\boldsymbol{D}$ and $\boldsymbol{E}$, $\boldsymbol{J}$ and $\boldsymbol{E}$, and $\boldsymbol{B}$ and $\boldsymbol{H}$ can be represented in equations (5)– (7).

$$\boldsymbol{D} = \varepsilon \boldsymbol{E} \tag{5}$$

$$\boldsymbol{J} = \sigma \boldsymbol{E} \tag{6}$$

$$\boldsymbol{B} = \mu\boldsymbol{H} \tag{7}$$

where ε, σ, and μ are the permittivity, conductivity and permeability, respectively.

The non-invasive ERT system excites voltage signal and measure current signal at the detection electrodes. Therefore, the relationship on how the current signal propagates in the medium of interest is very important. Based on equation (3), if the equation is multiplied with divergence of each side, it becomes as shown in equation (8):

$$\nabla = (\nabla.\boldsymbol{H}) = \nabla.(\boldsymbol{J} + j\omega\text{D}) \tag{8}$$

Then, the divergence of the curl become identically zero, hence, the equation of continuity [13] as follow,

$$0 = \nabla.\boldsymbol{J} + \nabla.j\omega\boldsymbol{D} \tag{9}$$

Substituting equation (5), equation (6), and $\boldsymbol{E}$ into equation (9), the equation of sensing field in the non-invasive ERT system can be shown in equation (10) and known as Poisson-type differential equation.

$$\nabla.(\sigma + j\omega\varepsilon)\nabla V = 0 \tag{10}$$

Thus, the non-invasive ERT system is based on the σ and relative permittivity, ε, (see equation (10)). The ω is the angular frequency of the excitation source. Moreover, the specific boundary condition of the sensing field of a non-invasive ERT system in two dimensions can be obtained by using equation (11).

$$
\begin{aligned}
\nabla.\big(\sigma(x,y) + j\omega\varepsilon(x,y)\big)\nabla(x,y) = 0 \qquad & (x,y) \subseteq \Omega \\
V_i(x,y) = V_o \qquad & (x,y) \subseteq \Gamma_i \\
V_j(x,y) = 0 \qquad & (x,y) \subseteq \Gamma_j \\
\frac{dV(x,y)}{dn} = 0 \qquad & (x,y) \subseteq \Gamma_k, (k \neq i,j)
\end{aligned}
\tag{11}
$$

Γi and Γj represent the spatial locations of n electrodes; i and j are the indexes of excitation and detection electrodes severally, and *Vo* is that the voltage applied to the system. Based on

Ampere's law, if considering the integral type, we have a tendency to get the entire current equation on the surface of the sensing field [14] as in equation (12):

$$\oint_c \boldsymbol{H}\, dl = \oint_s \boldsymbol{J}\, ds + \oint_s \frac{d}{dt}\boldsymbol{D}\, ds = I_c + I_d = I \tag{12}$$

where

I = total current on the surface,

I_c = conduction current,

I_d = displacement current,

s = surface of the electrode, and

d_s = discrete element of the electrode.

4. Methodology

The methodology in this paper only focus on the three dimensional of the simulation of using COMSOL Multiphysics software.

4.1 Modeling using COMSOL Multiphysics Software

For this paper, a specific set-up was done for each of the simulations. There were three main simulations had been conducted to investigate the sensor behaviour. The simulations were in term of sensor shapes, sizes and fringe effect. Here, the specific steps for all simulations were as follow:

1) Create a physical model using available geometries:

An acrylic pipe is used as the insulating pipe with outer diameter, thickness and length of the pipe are 100 mm, 2 mm and 200 mm, respectively. Here, the main concern is the sensor sensitivity. This means that, if the user gave the voltage signal to the electrode, it would allow the electricity to penetrate through the insulating pipe.

The 3D geometry of the non-invasive ERT system with two electrodes denote the electrodes applied in the system. Based on Ref. [4][15], an ideal size of the electrode is between 20-80% covering the inner surface of the pipeline. The cylinder pipe chosen would cause implementation of a formula of 360°/N, with N as the number of electrodes. It was used as the main formula for choosing the width dimension. This means that the width would be in terms of the electrode angle.

Besides, for 16 electrodes, formula for width for rectangular and circle shapes of ERT sensor were based on the formula in equation (13) and (14), respectively. Here, 75% covering size was applied for both shape of ERT sensor. The 75% covering size is equivalent to the 235.62mm in width for 16 electrodes. It means that, it would cover 14.73mm in width for each of sixteen electrodes attached to the pipe.

$$W_r = \frac{75}{100} \cdot 2\pi r / 16 \tag{13}$$

$$W_c = \frac{75}{100} \cdot 2\pi(50) / 16 \tag{14}$$

where

W_r = width for rectangular electrode

W_c = width for circle shape

r = inner radius of the pipe

Moreover, the system used here consists of a sensor with 16 measurement electrodes and two sets of driven guards. The shielding around sensor with size 2mm was put around each of the electrodes and it was set to the ground. The main effect of the grounded shield is to confine the field lines among the pipe, in order that they cannot travel from the supply electrode to the measuring electrode through the pipe wall as Ref. [16].

The 3D geometry of the non-invasive ERT system with one pair electrodes and different sizes of electrodes are shown in Figure 1 till Figure 3. The edges represent the vertical non-conducting pipe implemented in the real hardware.

(a)   (b)
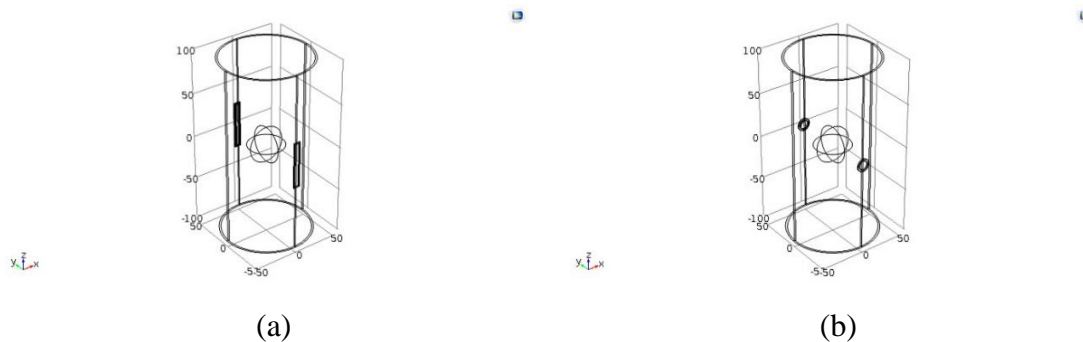
Figure 1. One pair of the measurement electrodes for non-invasive ERT for 25% out of the length pipe; (a) rectangular and (b) circle.

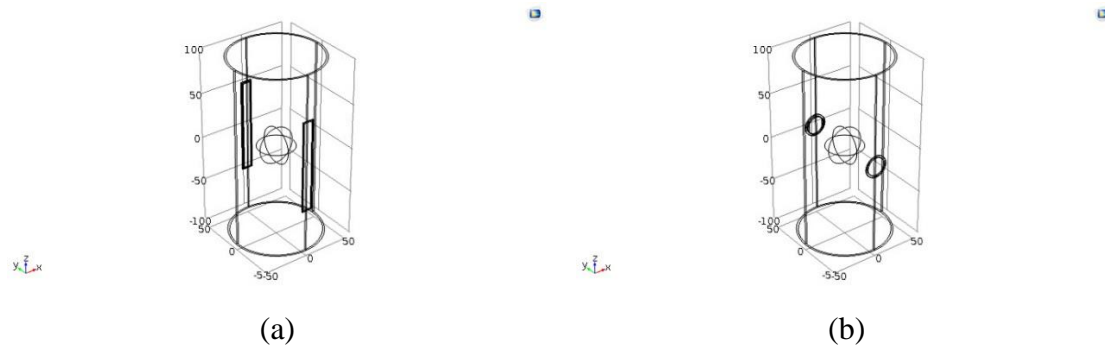(a)   (b)

Figure 2. One pair of the measurement electrodes for non-invasive ERT for 50% out of the length pipe; (a) rectangular and (b) circle.
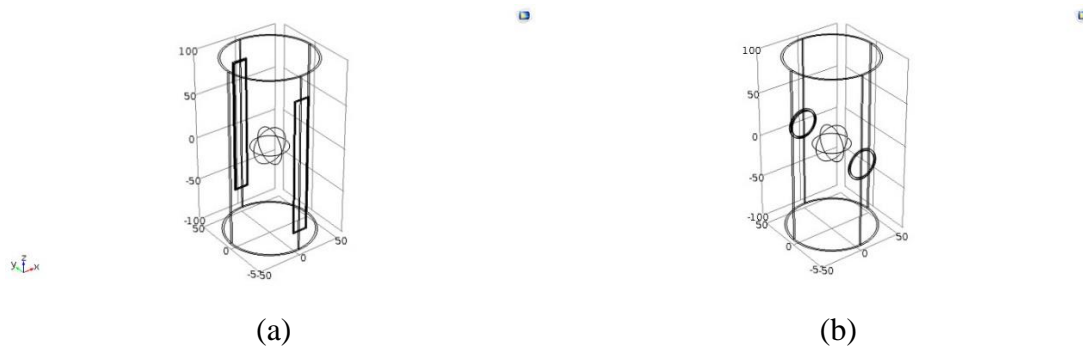

(a)   (b)

Figure 3. One pair of the measurement electrodes for non-invasive ERT for 75% out of the length pipe; (a) rectangular and (b) circle.

2)   Define materials for each domain created:

The geometry in three dimensions was drawn in step with the dimensions. The material for each of the domains was defined. This means that the real implementation of materials and pipe specifications assigned in COMSOL would influence the next steps of getting the results of the electrode dimensions. The conductive medium inside the vessel was water, and the insulating pipe was acrylic. the worth of the electrical physical phenomenon of H2O was mirrored with measured real tap water employed in the important hardware, employing a conductor meter and alternative materials, based on [4]. Table 1 shows the detail of parameter materials utilized in the project.

Table 1. Parameter set in COMSOL Multiphysics software

Material	Electrical conductivity (S/m)	Electrical permittivity
Acrylic	3.0×10^{-14}	3.45
Water	7.0×10^{-3}	80
Copper	5.998×10^{7}	1
Air	0	1

3)   Set the boundary condition for each of the electrodes

For the boundary setting, the boundary condition for the excitation electrode was set to the electric potential and the ground for the detection electrode. This boundary condition was set according to Maxwell's equation [4]. Based on equation (11), the electric potential was set at 10 V dc at electrode 1 and electrode 2 was set as the ground. The purpose for setting 10 V dc was because the frequency of the system was already defined in the frequency domain solver, so that the ac signal, like a sine waveform signal, was no longer necessary. Here, the frequency was set to 2MHz. However, there was a limitation on the frequency used, as it must correspond with the conductive liquid being used which only a conductivity range was between 5×10^{-3} S/m to 8×10^{-3} S/m. Despite that, the ac signal should be used for the real experiment. The mesh for the system was generated. Here, a normal mesh was chosen. Finally, the study was computed to get the result, and the capabilities of post-processing in COMSOL were applied.

4)   Mesh the model

For the simulation process, meshing the model could be crucial in obtaining the best result in a faster way. Thus, extremely fine meshing (Figure 4) under physically controlled mesh was chosen since denser meshing would provide a more reliable finite element method (FEM) simulation.

5)   Analyse the 3D result

Lastly, the 3D performance of the result obtained was selected according to the user. The analysis of the model was done by observing the Multislice plot, streamline plot and derived values was chosen for surface integration to find out current values. Below is expression for current:

$$I = ec.normJ*area\ of\ electrodes \qquad (15)$$

The Multislice plot for instance represents the electrical potential (V) distribution line and the electric field line distribution was obtained by using the streamline plot of the non-invasive ERT system.
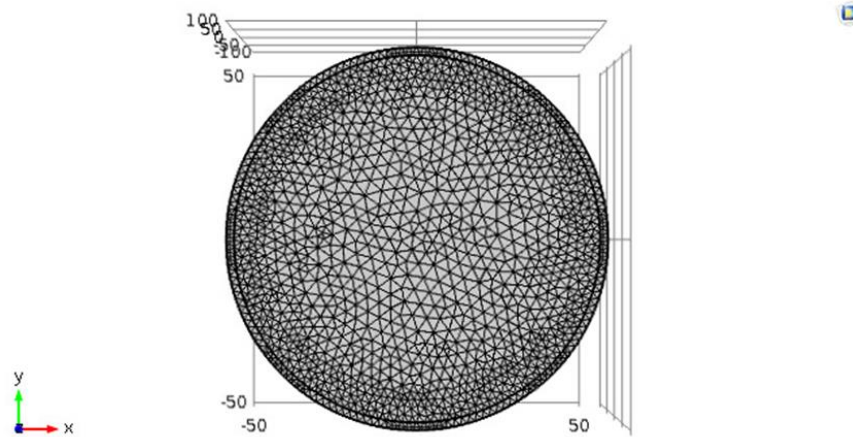

Figure 4. Extremely fine meshing model

5. Results and Discussion

The results from the simulation have been divided into several parts: different sizes, shapes and fringe effect. Here, the project only focusses on one pair of electrodes. The obstacle of air with 40 mm in diameter at the center of the pipe was applied to observe the electrical signal propagation in the pipe.

5.1 Different Shapes and Sizes of ERT sensor

The results of circle shape were presented in Table 2. The sensor readings performance for each percentage of covering size were shown in Table 3.

Table 2. Circle shape with presence of gas
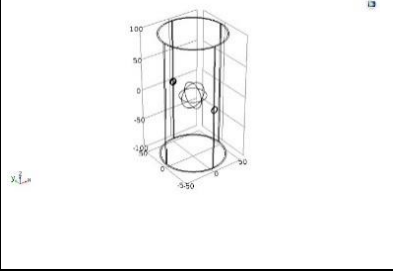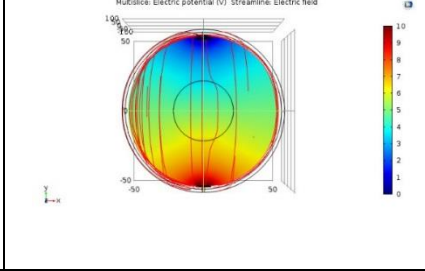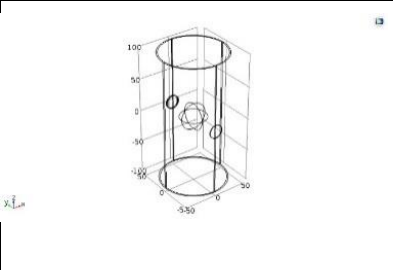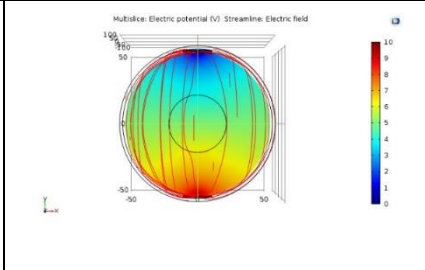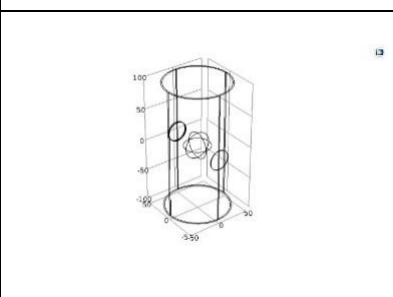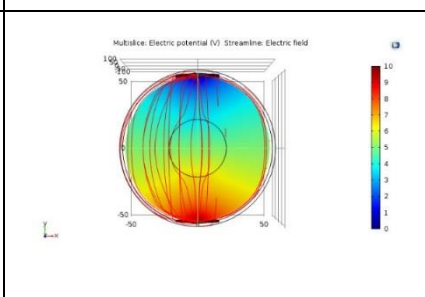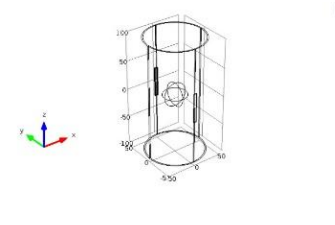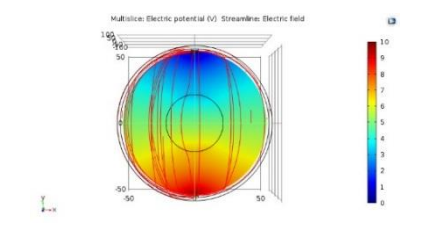
Size	Circle	
	3D Geometry	**Multislice & Streamline**
25%		
50%		
75%		

Table 3. Sensor Reading for circle shape

Size	Current (mA)
25%	6.59×10^{-3}
50%	47.68×10^{-3}
75%	178.21×10^{-3}

The result of rectangular were presented in Table 4. The sensor reading performance for each percentage of covering size were shown in Table 5.

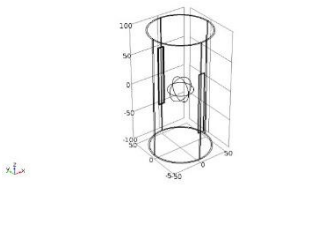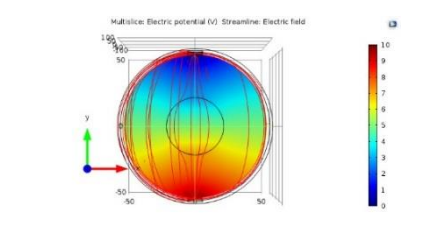**Table 4.** Rectangular Shape with presence of gas
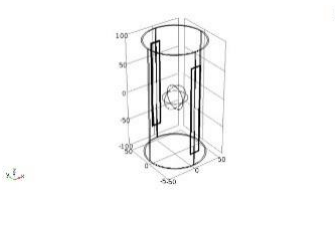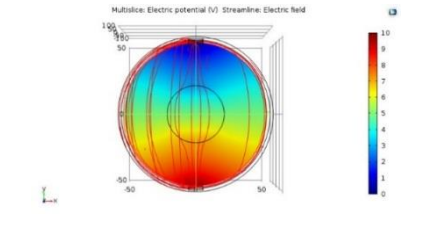
Size	Rectangular	
	3D Geometry	**Multislice & Streamline**
25%		
50%		
75%		

Table 5. Sensor Reading for rectangular shape

Size	Current (mA)
25%	20.59×10^{-3}
50%	270.76×10^{-3}
75%	162.51×10^{-4}

5.2 Shield versus Non-Shield of ERT Sensor

The shield versus non-shied of ET sensor were carried out to investigate the fringe effect of the ERT sensor. Table 6 presents the results for non-shield circle shape. The current value reading for each percentage of covering size was obtained in Table 7.
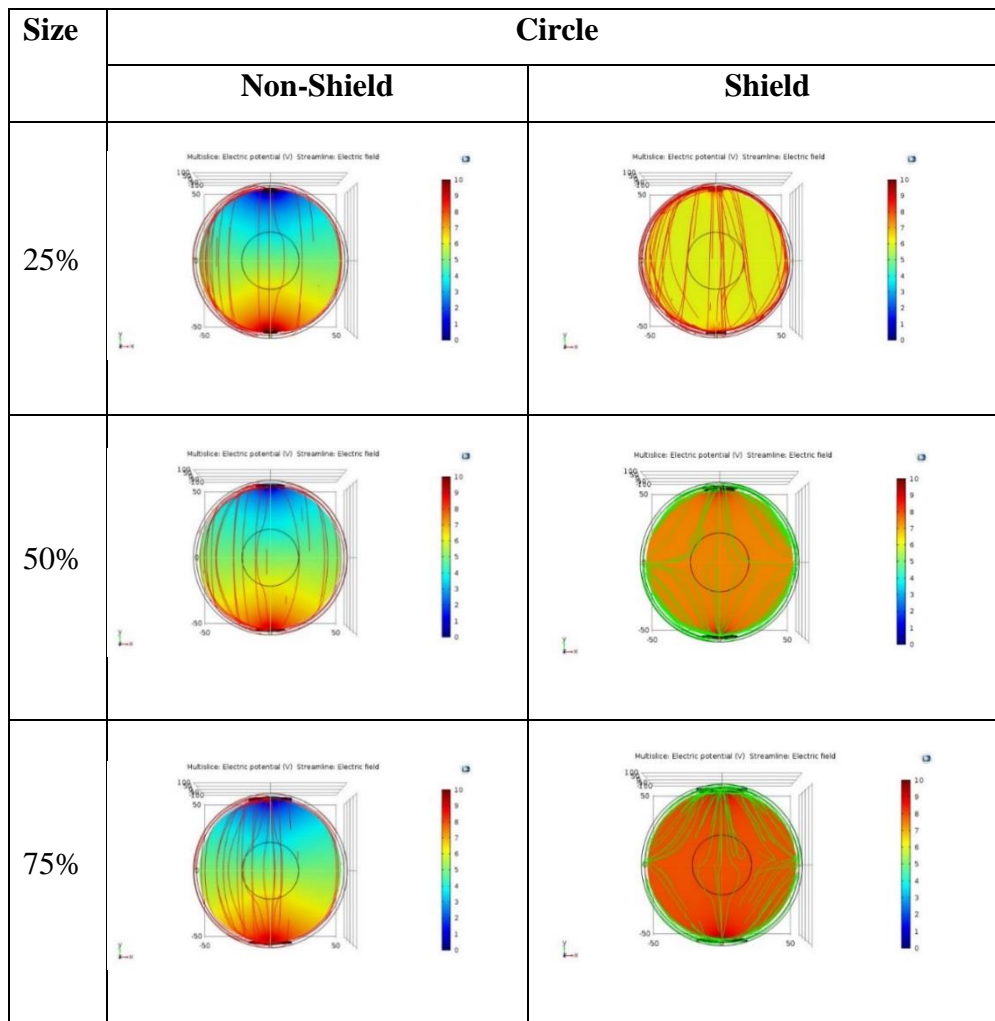
Table 6. Circle shape with copper material

Size	Circle	
	Non-Shield	**Shield**
25%		
50%		
75%		

Table 7. Current Reading for Circle Shape

Size	Non-shield (mA)	Shield (mA)
25%	6.59×10^{-3}	6.69×10^{-3}
50%	47.68×10^{-3}	57.04×10^{-3}
75%	178.21×10^{-3}	185.09×10^{-3}

The result for non-shield circle shape was illustrated in Table 8. The current value reading for each percentage of covering size was obtained in Table 9.
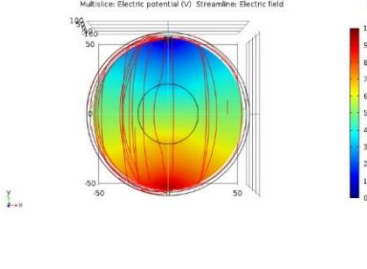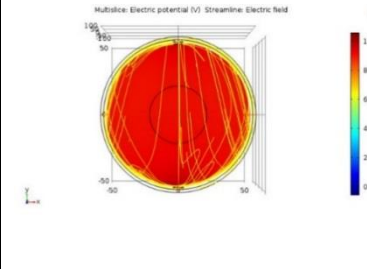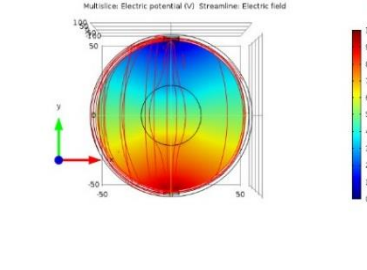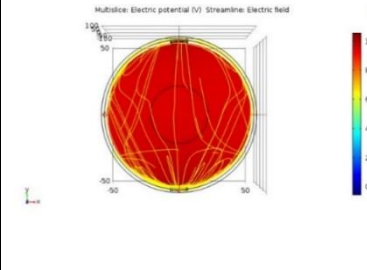
Table 8. Rectangular shape with copper material
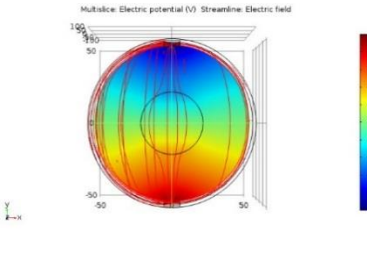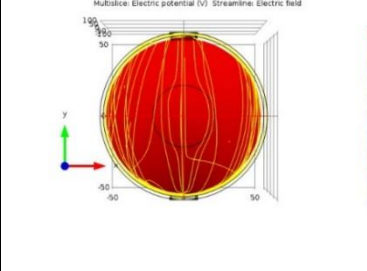
Size	Rectangular	
	Non-Shield	**Shield**
25%		
50%		
75%		

Table 9. Current Reading for Rectangular Shape

Size	Non-shield (mA)	Shield (mA)
25%	20.59×10^{-3}	7.26×10^{-3}
50%	270.76×10^{-3}	57.82×10^{-3}
75%	162.51×10^{-4}	144.14×10^{-3}

5.3   Analysis and Discussion

Based on the results of sizes and shapes of sensor between 25%, 50% and 75% in Table 2 till Table 5, there was a large gap between each percentage of the covering sizes. For distribution, it can be revealed that the 75% showed more electrical field distribution in the pipe. Moreover, the current value reading of 25% covering size presented the smaller current value compared to the 75% covering size. The simulation was performed in order to investigate the feasibility of the electrical field distribution from the excitation electrode through the acrylic pipe before

it received by the detection electrode. The voltage signal should penetrate the acrylic pipe and decrease gradually when it reaches the detection electrode. As the detection electrode was connected to the ground, later the current could be measured at the detection electrode.

In addition, as can be seen in Table 6 until Table 9, the field lines that travel from the source electrode through the pipe wall, crossing the equi-potential lines perpendicularly, stopped at the grounded axial tracks before they could reach at the measuring electrode. The external field lines were neutralized by the grounded screen. The electric field distribution along the Z axis also becomes distorted when grounded shielding was presented.

3. Conclusion

ERT sensor with size of 75% out of length pipe can be used as the optimize size for ERT sensor. Simulations for the fringe effect of ERT sensors with and without guards were also carried out with different length of the electrodes. It was concluded that ERT sensors with longer electrodes have less fringe effect. The grounded guards were applied in the ERT sensors and it was integrating together with the ERT sensors. Simulation results revealed that ERT sensors with grounded guards had less fringe effect. Multislice result shows a cross-sectional surface that indicate how a variable change over a distance or a specific area of the plot. It was believed that a further exploration and improvement of the ERT sensor can provide a broad alternative way to visualize and monitor the industry applications.

Acknowledgment

References

[1]   Y. Abdul Wahab *et al.*, "Non-invasive process tomography in chemical mixtures – A review," *Sensors and Actuators B: Chemical*, vol. 210, pp. 602–617, Apr. 2015, doi: 10.1016/j.snb.2014.12.103.

[2]   L. Liu, Z. Y. Fang, Y. P. Wu, X. P. Lai, P. Wang, and K. I. I. L. Song, "Experimental investigation of solid-liquid two-phase flow in cemented rock-tailings backfill using Electrical Resistance Tomography," *Construction and Building Materials*, vol. 175, pp. 267–276, 2018, doi: 10.1016/j.conbuildmat.2018.04.139.

[3]   W. Na *et al.*, "Imaging of gas-liquid annular flows for underbalanced drilling using electrical resistance tomography," *Flow Measurement and Instrumentation*, vol. 46, pp. 319–326, 2015, doi: 10.1016/j.flowmeasinst.2015.07.003.

[4]   Y. Abdul Wahab *et al.*, "Optimisation of electrode dimensions of ERT for non-invasive measurement applied for static liquid–gas regime identification," *Sensors and Actuators, A: Physical*, vol. 270, pp. 50–64, 2018, doi: 10.1016/j.sna.2017.12.017.

[5]   C. R. Carrigan *et al.*, "Electrical resistance tomographic monitoring of CO2movement in deep geologic reservoirs," *International Journal of Greenhouse Gas Control*, vol. 18, pp. 401–408, 2013, doi: 10.1016/j.ijggc.2013.04.016.

[6]   J. Boaga, M. Rossi, and G. Cassiani, "Monitoring Soil-plant Interactions in an Apple Orchard Using 3D Electrical Resistivity Tomography," *Procedia Environmental Sciences*, vol. 19, pp. 394–402, 2013, doi: 10.1016/j.proenv.2013.06.045.

[7]   D. A. Gunn *et al.*, "Moisture monitoring in clay embankments using electrical resistivity tomography," *Construction and Building Materials*, vol. 92, pp. 82–94, 2015, doi: 10.1016/j.conbuildmat.2014.06.007.

[8]   C. Carletti, G. Montante, C. De Blasio, and A. Paglianti, "Liquid mixing dynamics in slurry stirred tanks based on electrical resistance tomography," *Chemical Engineering Science*, vol. 152, pp. 478–487, 2016, doi: 10.1016/j.ces.2016.06.044.

[9]   B. Wang, Y. Hu, H. Ji, Z. Huang, and H. Li, "A Novel Electrical Resistance Tomography System Based on C4D Technique Technique," *IEEE Transactions on Instrumentation and Measurement*, vol. 62, no. 5, pp. 1017–1024, 2013.

[10]   Z. Ye, H. Y. Wei, and M. Soleimani, "Resolution analysis using fully 3D electrical capacitive tomography," *Measurement: Journal of the International Measurement Confederation*, vol. 61, pp. 270–279, 2015, doi: 10.1016/j.measurement.2014.10.060.

[11]   N. Hashemi, F. Ein-Mozaffari, S. R. Upreti, and D. K. Hwang, "Experimental investigation of the bubble behavior in an aerated coaxial mixing vessel through electrical resistance tomography (ERT)," *Chemical Engineering Journal*, vol. 289, pp. 402–412, 2016, doi: 10.1016/j.cej.2015.12.077.

[12]   D. K. Kalluri, "Quasistatic and Static Approximations," *Principles of Electromagnetic Waves and Materials*, pp. 11–16.

[13]   J.Larsson, "Electromagnetics from A Quasistatic Perspective," *American Journal of Physics*, vol. 75, no. 3, p. 230, 2006, doi: 10.5772/64434.

[14]   and U. R. F. T. Ulaby, E. Michielssen, "Displacement Current," *Fundamentals of Applied Electromagnetics*, vol. 6th ed, pp. 299–300, 2010.

[15]   T. D. Machin, H. Y. Wei, R. W. Greenwood, and M. J. H. Simmons, "In-pipe rheology and mixing characterisation using electrical resistance sensing," *Chemical Engineering Science*, vol. 187, pp. 327–341, 2018, doi: 10.1016/j.ces.2018.05.017.

[16]   J. A. P. and J. L. F. M. A. Martinez Olmos, "Influence of Shielding Arrangement on ECT Sensors," *MDPI*, pp. 1118–1127, 2006.